

Article

The Law and Mechanism of the Effect of Surface Roughness on Microwave-Assisted Rock Breaking

Fangfang Chen ¹, Guoqing Li ^{1,*}, Zhiqiang Zhang ² and Zhanqiang Wu ¹

¹ School of Architecture and Civil Engineering, Xi'an University of Science and Technology, Xi'an 710054, China; chenff@xust.edu.cn (F.C.); wuzq@stu.xust.edu.cn (Z.W.)

² School of Civil Engineering and Architecture, Xi'an University of Technology, Xi'an 710048, China; zhangzq87@xaut.edu.cn

* Correspondence: 21204053034@stu.xust.edu.cn

Abstract: In physical engineering, a rock surface, whether naturally or artificially formed, is rough. When irradiating rocks, microwaves produce reflections and diffractions on the surface of rough rocks, which significantly affect the absorption of microwave energy by rocks, thus influencing the result of microwave irradiation. In order to explore the influence of rough rock surfaces on the effect of microwave-assisted rock breaking, microwave irradiation tests were carried out on basalt samples with different values of roughness to test the temperature and P-wave velocity of the samples before and after microwave irradiation. Numerical test methods were used to systematically study the influence of rough rock surfaces on microwave irradiation. The results show that, under the same microwave irradiation conditions, the effect of microwave irradiation on rough surface basalt is more significant than that of flat surface basalt. The surface temperature distribution range of flat surface specimens is narrow, the surface temperature range of rough surface specimens is wider and more inhomogeneous, and the maximum surface temperatures of rough surface specimens are much higher than those of flat surface specimens. After irradiation, new macroscopic cracks were generated on the surface of the samples, and the crack propagation of the rough surface samples was more obvious. The decrease in P-wave velocity before and after the irradiation of flat surface samples is small, and that of rough surface samples is larger. The main factors affecting the effect of microwave irradiation on the rough surface are the refraction and reflection of electromagnetic waves, heat conduction, and stress concentration on the surface.

Keywords: microwave irradiation; surface roughness; crack propagation; thermal stress; thermal conduction



Citation: Chen, F.; Li, G.; Zhang, Z.; Wu, Z. The Law and Mechanism of the Effect of Surface Roughness on Microwave-Assisted Rock Breaking. *Appl. Sci.* **2024**, *14*, 207. <https://doi.org/10.3390/app14010207>

Academic Editor: Nikolaos Koukouras

Received: 30 November 2023

Revised: 18 December 2023

Accepted: 22 December 2023

Published: 26 December 2023



Copyright: © 2023 by the authors. Licensee MDPI, Basel, Switzerland. This article is an open access article distributed under the terms and conditions of the Creative Commons Attribution (CC BY) license (<https://creativecommons.org/licenses/by/4.0/>).

1. Introduction

Hard-rock excavation has been a key problem in underground space excavation and resource exploitation, and it has been the focus of study by many scholars for a long time. Traditional rock underground space excavation is mainly performed using the drilling and blasting methods and the mechanical method [1,2]: The drilling and blasting methods induce large disturbances in the original rock, which can easily cause damage to the surrounding rock, and have low construction accuracy. With the rapid development of mechanical excavation, the mechanical method has overcome the deficits of most drilling and blasting methods, but it still exhibits large wear and low efficiency when excavating hard rock. Therefore, the development of an energy-saving, efficient, and economical hard-rock crushing method is a necessary part of the development of underground engineering excavation technology [3]. The strength of rock is significantly weakened after microwave irradiation; thus, some scholars have proposed the application of microwave radiation to mechanical rock breaking with many studies having demonstrated significant results.

Microwave heating has the characteristics of bulk heating, rapid speed heating, energy saving, high efficiency, easy control, and safety. Microwave irradiation can be used as an

auxiliary means of rock breaking and applied to hard-rock excavation engineering [4,5]. Some preliminary research results on microwave-assisted rock breaking are as follows: Bai et al. [6–8] explored the mechanism of microwave radiation damage to rocks and found that the higher the mineral iron content in the rock, the more serious the rock damage after microwave irradiation; Hu et al. [9–11] found that the microwave irradiation power and irradiation time are the main factors affecting the damage and strength weakening of the internal structure of rocks, and when the power increases to a certain extent, the influence of irradiation time on the strength of rock and the weakening degree of the internal structure is gradually significant; Chen et al. [12,13] studied the effect of microwave heating pathways on the effect of microwave radiation on rock and found that, when the microwave energy input was consistently maintained, the rock-breaking effect was better when following the irradiation pathway of ‘first low and then high’; Lu et al. [14,15] found that the response of rocks to temperature increases under microwave irradiation was mainly related to the dielectric properties and mineral content of the rocks themselves; Liu et al. [16,17] found that the effect of microwave irradiation can be improved by increasing the water content of rock mass, but the effect will decrease with an increase in water content; Zhang et al. [18–20] found that, under different stress conditions, a complex crack network dominated by tensile cracks was generated in the rock samples after microwave-induced borehole rupture under different stress conditions, and the thermal fracture process could be divided into a silent period, calm period, dense period, and continuous period; Chen et al. [21–23] found that the microwave irradiation law of different irradiation distances decreased when the irradiation distance increased. The microwave irradiation surfaces of the rock samples in the abovementioned studies were set to be flat and smooth, which is inconsistent with actual engineering situations. At present, research on the laws and mechanisms of the effect of microwave irradiation on rough rock surfaces is still lacking.

The tunnel boring machine (TBM) creates rough rock surfaces, which will inevitably influence the microwave irradiation effect. In previous studies, the sample surfaces were assumed to be smooth and flat, which is far from the actual engineering scenario. In the author’s preliminary experiments, it was found that rough rock surfaces have a certain influence on the effect of microwave-assisted rock breaking. Obvious differences are observed in the electric field distribution, temperature rise characteristics, crack evolution, and plastic zone distribution between flat surfaces and rough surfaces under microwave irradiation as well as disparities in the effect of irradiation on different roughness degrees. In this study, basalt was taken as the research object, and microwave-irradiation tests of rock samples with different surface roughness values were carried out. The influence of rock surface roughness on the effect of microwave irradiation was analyzed from the aspects of temperature characteristics, crack evolution, and P-wave wave velocity so as to reveal the mechanisms of microwave reflection, diffraction, absorption, and rock failure on the surface of rocks with different roughness values, which is of great significance for the practical application of microwave-assisted rock-breaking technology.

2. Effect of Roughness on the P-Wave Velocity and Crack Propagation of the Specimen

2.1. Characterization of Rock Surface Roughness

It has been found that the surface roughness of rock has a certain influence on its shear strength [24,25]. Therefore, the research on the characterization method of rock surface roughness has been relatively perfect.

Many methods can be used to characterize the surface roughness of rocks, such as the comparison method, straight edge method, and contour rms method. According to the test method and cost considerations, the EL Soudani roughness quantitative characterization method [26] was selected in this study, as shown in Equation (1), i.e., the contour roughness R_p calculation:

$$R_p = \frac{L_p}{L} \quad (1)$$

where R_p is the roughness of the rock surface contour line, L_p is the actual length of the contour line of the rock surface (m), and L is the length of the contour line of the rock surface (m).

2.2. Test Specimen

Basalt is an extremely hard rock, which is mainly composed of basic feldspar, pyroxene, and olivine. Pyroxene is a strongly microwave-absorbing mineral; olivine is a moderately microwave-absorbing mineral; and feldspar is a non-microwave-absorbing mineral. The basalt used in this paper was taken from Chifeng, Inner Mongolia. The sample size was 100 mm × 100 mm × 30 mm, and the surface of the sample was a natural surface, as shown in Figure 1. Some of the physical and mechanical parameters of basalt are shown in Table 1 (all measured in the Mechanics Laboratory of Graduate School of Xi'an University of Science and Technology). The P-wave velocity is measured with an NM-4A non-metallic ultrasonic testing analyzer, and the compressive strength (ISRM) is measured with a TYA-2000 digital display pressure testing machine (Shenrui, Shanghai, China).

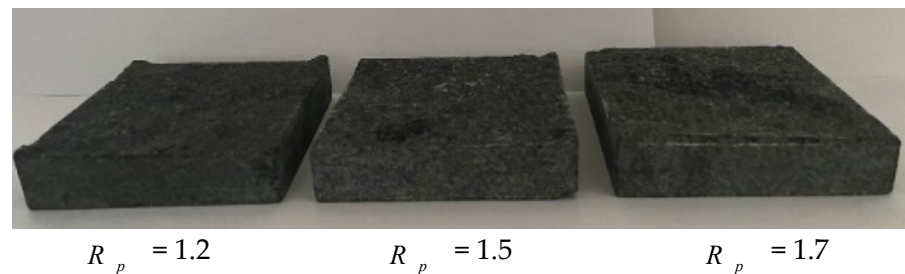


Figure 1. The surface of the basalt samples.

Table 1. Physical and mechanical parameters of basalt.

P-Wave Velocity ($\text{m}\cdot\text{s}^{-1}$)	Density ($\text{g}\cdot\text{cm}^{-3}$)	Compressive Strength (MPa)
5556~5952	2.95	245

2.3. Test Equipment

A commercial EMB17G4V-SS microwave system (Midea Group, Foshan, China) was used in the test, which has a single-mode resonator with a microwave frequency of 2.45 GHz. To simulate one-sided irradiation, silicon carbide plates were placed around and on the bottom surface of the microwave oven for processing, as shown in Figure 2. Silicon carbide plates have a strong ability to absorb microwaves [27,28] and can, thus, absorb most of the microwaves and achieve single-sided irradiation [5].

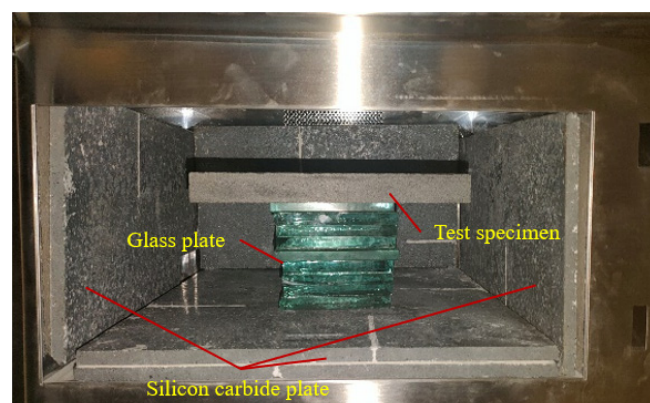


Figure 2. Arrangement of the microwave oven irradiation chamber.

2.4. Scheme and Process

The test sample was divided into 3 groups—A, B, and C—with 8 samples in each group: One sample with a smooth surface and 7 samples with different roughness values. Specimens A-1 to A-7 had roughness values of 1.1 to 1.7, respectively; Figure 1 shows samples A-2, A-5, and A-7. Microwave irradiation was carried out before the experiment; the microwave irradiation power was finally selected as 1 kW, and the irradiation time was 180 s. The test process was followed to measure and calculate the surface roughness of the sample, perform ultrasonic wave velocity tests on the sample, conduct real-time temperature measurements after irradiation, and then carry out the ultrasonic wave velocity test. The method of measuring and calculating the surface roughness was as follows. A needle-comb-type contour extractor was used to extract the surface contour line of the specimen with an upper surface size of the sample being 100 mm × 100 mm. In order to extract the contour line uniformly, 11 contour lines were extracted longitudinally; the spacing of adjacent contour lines was 10 mm, as shown in Figure 3a. The length of each contour was calculated using MATLAB (2020b), and the average roughness of all contour lines calculated using Equation (1) for each specimen was used as the surface roughness of the specimen, as shown in Figure 3b.

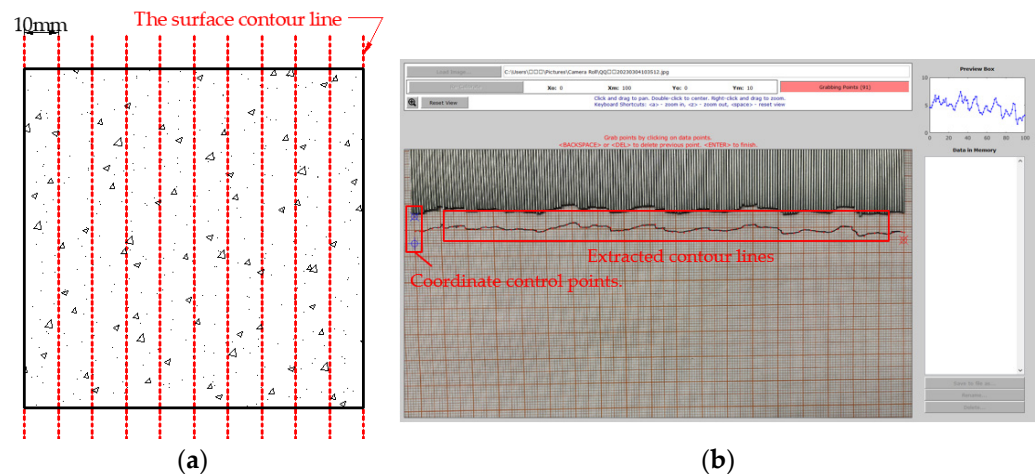


Figure 3. Measurement and calculation of surface roughness. (a) Contour line extraction. (b) Roughness calculation.

2.5. Results

2.5.1. Temperature Distribution

Figure 4 show the surface temperature distributions of a flat smooth surface and partially rough surface specimens, respectively. The high-temperature zone of the flat smooth surface was concentrated in the center of the sample, which was approximately circular, and the high-temperature distribution area was small. The peak surface temperature was 123 °C. The high-temperature area on the surface of the 1.5 roughness specimen was irregularly shaped and covered a large distribution area; the peak temperature was 213 °C. The surface profile and temperature distribution of the rock sample indicate that the shape of the temperature distribution has a certain relationship with the undulating profile of the sample, and the surface temperature peak occurred at the convex contour position.

Figure 5 shows the curve of the peak surface temperature of the sample as a function of roughness. The peak temperature of the flat surface sample was 123 °C, and the peak temperature gradually increased with the increase in roughness. When the roughness reached 1.5, the growth rate decreased, and the temperature peaks of all rough surfaces were much greater than those of flat surfaces.

Figure 6 shows the curve of the average surface temperature of the sample with roughness after MATLAB image post-processing. When the roughness was less than 1.5, the average surface temperature of the sample increased with the increase in roughness.

When the roughness was greater than 1.5, the average temperature decreased slowly, and a threshold between roughness values of approximately 1.4 and 1.6 promoted the maximum average temperature. The surface temperature distribution of the sample indicated that the main surface temperature distribution areas of samples with roughness values greater than 1.5 (A-7 and C-7 specimens in Figure 4) were discontinuous, showing the distribution of local high temperature. The high-temperature area decreased, and the surface area of the samples increased with the increase in roughness, resulting in decreases in the average temperature of the whole surface. The average temperature of the flat surface was approximately 74 °C, and the average maximum temperature of the rough surface was 112 °C, representing an increase of approximately 51.4%. Thus, the effect of microwave irradiation on rough surface samples was better.

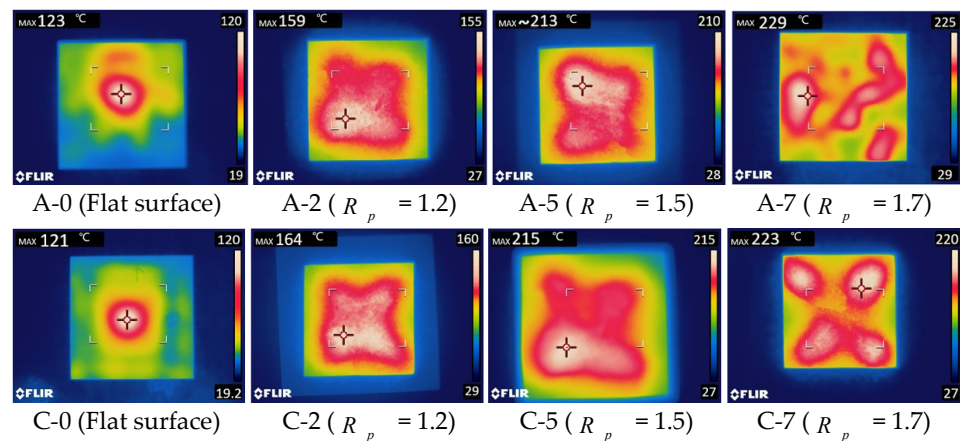


Figure 4. Temperature distribution of some rough surface samples.

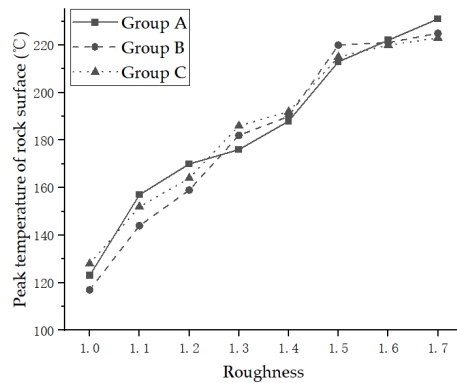


Figure 5. Peak temperature values of the samples as a function of roughness.

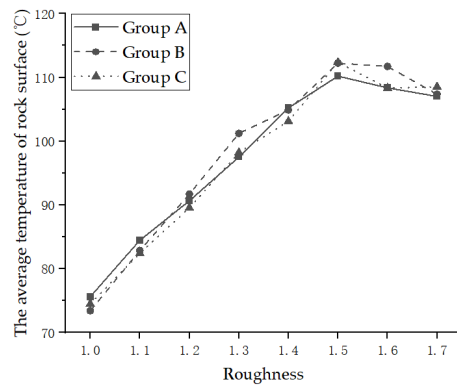


Figure 6. Variation curve of the average temperature of the sample with varying roughness values.

2.5.2. Crack Growth

The dielectric properties and thermal expansion coefficients of each mineral in basalt are different; therefore, basalt expands unevenly after microwave irradiation, resulting in cracks. Before irradiation, there were no macroscopic cracks on the surface of the flat specimen, and no macroscopic cracks were observed on the surface of the specimen after microwave irradiation. However, there was significant crack propagation on the surface of the rough specimen. During the microwave irradiation, the local temperature of the rough surface was higher, and the temperature distribution was uneven, so the local position generated large thermal stress; then, new cracks were generated when the rock strength limit was exceeded. The crack of the rough surface specimen is shown in Figure 7. The above shows that the microwave irradiation effect of a rough rock surface is better, which is beneficial to improve the efficiency of microwave-assisted rock breaking.

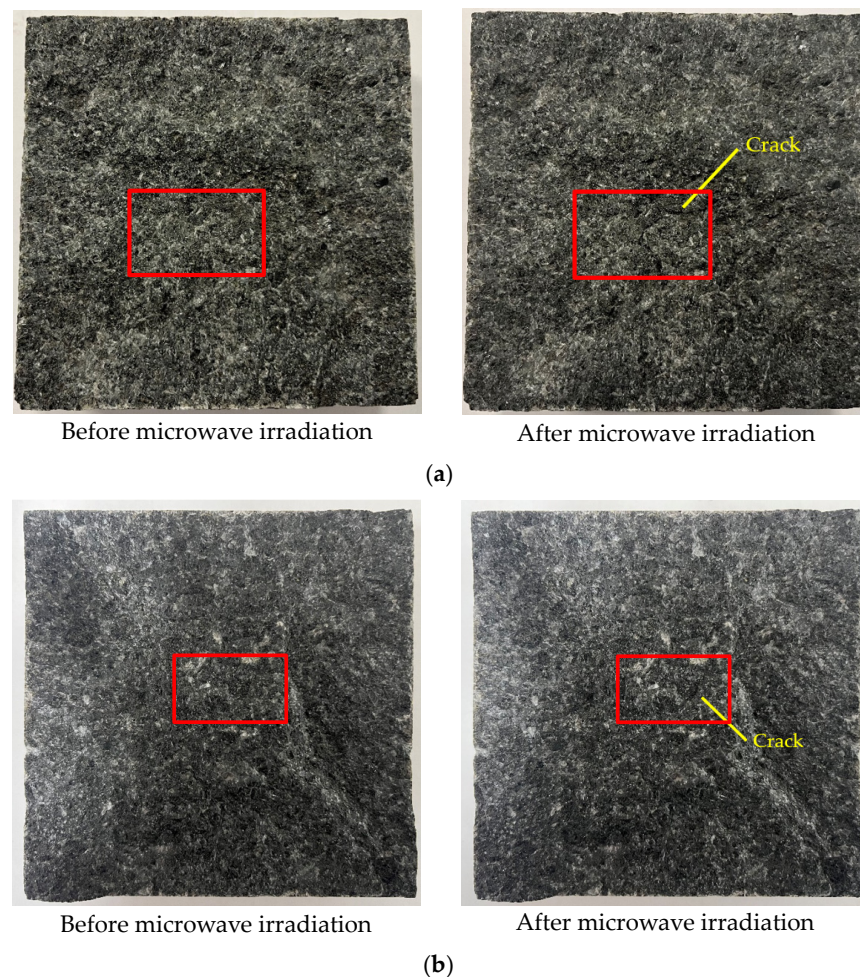


Figure 7. Surface crack propagation after microwave irradiation of the specimen. (a) A-3. ($R_p = 1.3$). (b) C-5. ($R_p = 1.5$).

2.5.3. P-Wave Velocity

Non-metallic ultrasonic detectors were utilized to detect the degree of damage to the test sample after microwave irradiation. The P-wave velocities of group A samples before and after microwave irradiation are shown in Figure 8. The P-wave velocities of all samples decreased after microwave irradiation, the wave velocity of the flat surface specimen decreased by approximately 2%, and the wave velocity decreased first and then decreased with the increase in roughness. The samples with the largest reduction in wave velocity in groups A, B, and C were specimens 1.5, 1.5, and 1.4, respectively, with wave velocity reductions of 7.2%, 7.0%, and 8.4%, respectively. Under the same irradiation

conditions, the temperature of the leveled basalt sample was lower, the thermal stress was smaller, and the damage was diminished. The temperature distribution of the rough surface specimens was uneven, and the undulating contours led to greater thermal stress at local high temperatures, resulting in more induced damage.

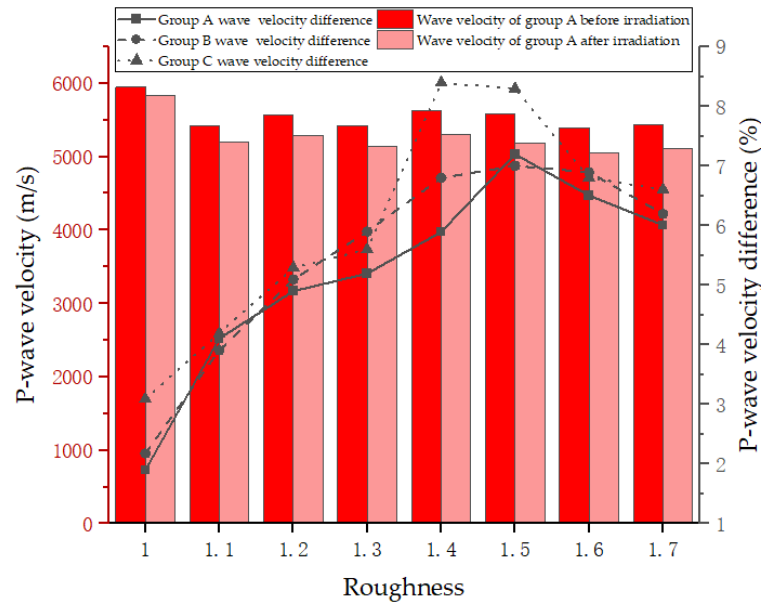


Figure 8. P-wave velocities and wave velocity differences of the samples before and after irradiation.

3. Numerical Experiment

3.1. Modelling

In order to study the influence of roughness on the effect of microwave-assisted rock breaking more systematically, the electromagnetic field, temperature distribution, and plastic zone were analyzed through numerical tests so as to make up for the shortcomings of physical tests in determining key characteristics, such as the electromagnetic field and plastic zone.

The numerical model was the same size as the rock sample, as shown in Figure 9. The selected physical and mechanical parameters were derived from the existing literature [29,30]. The 11 contour lines were imported into MATLAB to extract the data points and then imported into COMSOL5.6 to generate an equiscale model. Finally, electromagnetic–thermal–mechanical coupling calculations were performed to analyze the electric field contours, temperature fields, and plastic zone distributions. The microwave frequency, irradiation power, and irradiation time are consistent with the physical test. The boundary conditions were consistent with the physical test, the mechanical boundary was the fixed-end bottom surface, and the surrounding and top surfaces were the free ends. The electromagnetic boundary condition was that the side surface and the bottom surface were the scattering boundary.

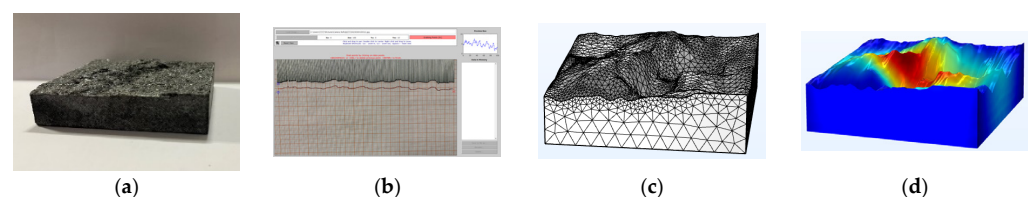


Figure 9. Numerical model building process. (a) Rock sample. (b) Contour extraction, calculation of roughness, extraction of data points. (c) Mesh. (d) Cloud diagram of the temperature, electric field, and plastic zone was obtained.

3.2. Electromagnetic Field Characteristics

Figure 10 depicts the electric field cloud diagram of each sample, indicating that the electric field intensity decreased outward from the center of the sample; the electric field distribution of the rough surface sample was more concentrated than that of the flat surface sample, and the maximum electric field intensity was larger. The peak value of the electric field intensity increased first and then decreased with the increase in roughness, and the peak value of the electric field reached the maximum when the roughness value was 1.4~1.6. The differences between the peak electric field of the samples with roughness values of 1.1~1.7 and those with a flat surface were 19.0%, 22.1%, 24.6%, 25.3%, 29.9%, 26.2%, and 23.6%, respectively. The peak electric fields of the samples with roughness values of 1.1 to 1.5 increased by 10.9%, and the peak electric field difference between the specimen with a roughness value of 1.4 and that with a roughness of 1.5 was the largest: 4.6%. As shown in Figure 11, the average electric field intensity of the rock surface increased first and then decreased with the increase in roughness. The average electric field of the specimen with a roughness of 1.5 reached the maximum, 3715 V/m, which was basically consistent with the change in electric field peak.

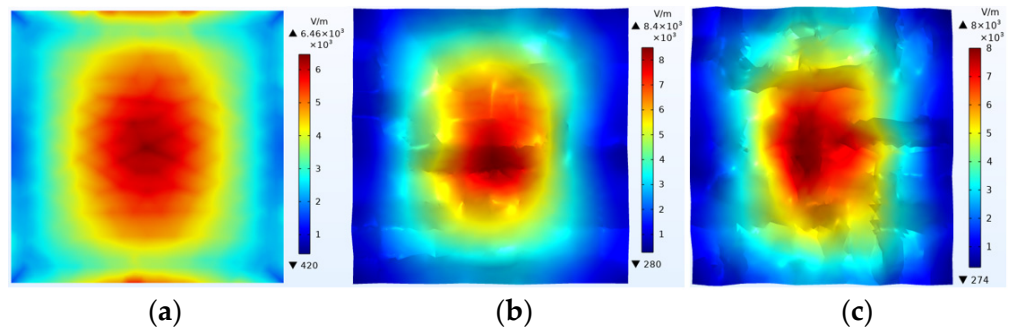


Figure 10. Electric field cloud diagrams of the surfaces of each sample (Group A). (a) Flat surface. (b) $R_p = 1.5$. (c) $R_p = 1.7$.

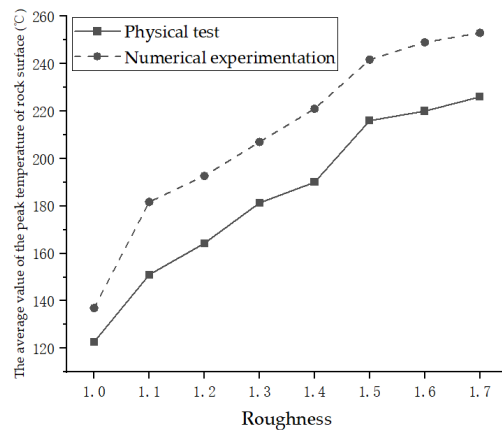


Figure 11. The average electric field strengths on the surfaces of samples with different values of roughness.

The above analysis shows that the surface roughness has a significant effect on the electric field distribution. As shown in Figure 12, in the same model, in the absence of rock samples, the peak electric field and average electric field intensities of the electromagnetic wave transmission at the same distance were 15000 V/m and 9021 V/m, respectively; the peak and average electric fields irradiated with electromagnetic waves on the surface of the flat rock were 56.9% and 66.9%, respectively, and the peak and average electric fields on the surface of the rough rock were 44.1~48.7% and 59.0~61.6%, respectively, which are much

smaller values than those on the surface of the flat rock. The rough surface reduced the loss of electric field strength and improved the effect of microwave irradiation on the rocks.

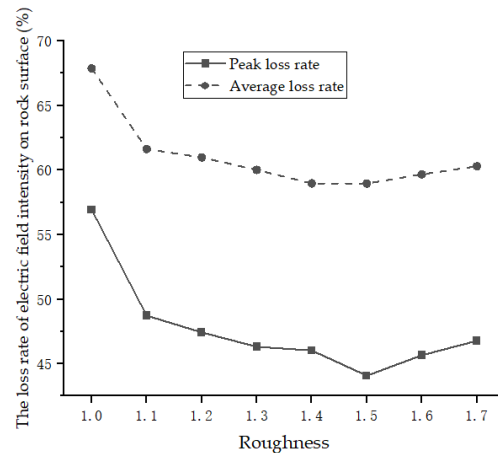


Figure 12. Loss rate of electric field strength on the surfaces of samples with different values of roughness.

3.3. Temperature Distribution Characteristics

As shown in Figure 13, the average surface temperature of the specimen with a roughness value of 1.5 was the largest, 19.8% higher than that of the sample with the flat surface. Figure 14 shows the average peak temperatures of each rock surface with varied roughness values in the physical test and the numerical experiment: The trends in peak temperature under the two types of tests were approximately the same, both increasing with the increase in roughness, and were significantly larger than that of the flat surface, and the peak temperature growth rates decreased above roughness values of 1.5. However, there was a certain gap between the average peak temperature value of the physical test and the numerical test. This was mainly due to the error caused by infrared thermography of the specimen.

There was a significant peak temperature difference between the sample with a flat surface and that with a roughness value of 1.1; moreover, the physical and numerical tests revealed peak rock surface temperatures of 231 °C and 249 °C, respectively, for the specimen with a roughness value of 1.7, which was approximately 1.9 times greater than that of the flat surface.

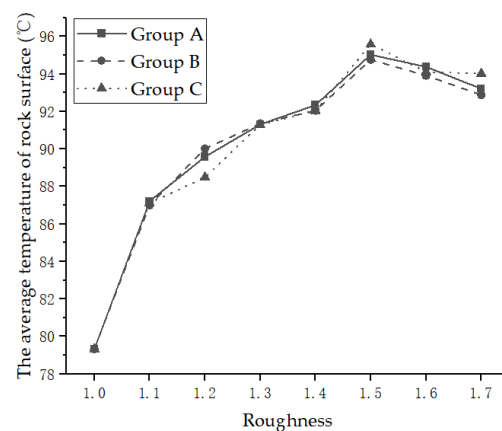


Figure 13. Average temperatures on the surface of samples with different values of roughness.

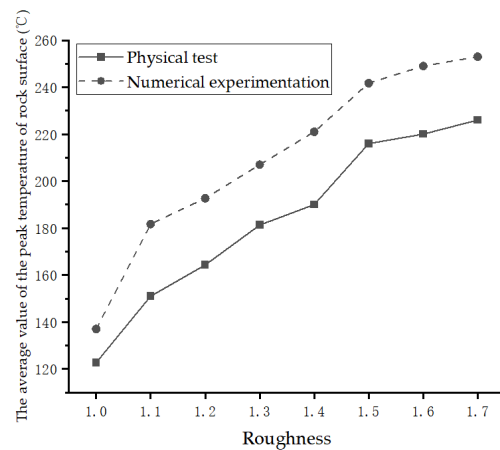


Figure 14. The average peak temperature values of the samples with different roughness values obtained through physical and numerical experiments.

3.4. Plastic Zone

The plastic zone is an important index for determining the effect of microwave irradiation, which is usually analyzed from the distribution and size of the plastic zone. There was no plastic zone on the surface of the flat rock, and the plastic zone of the rough rock surface was mainly distributed in the central area of the rock surface, which is basically consistent with the distribution of the temperature and electric field. The plastic zone of the sample with a roughness of 1.2 was roughly distributed in the central area of the rock surface, and the plastic zone of the specimen with a roughness 1.5 was mainly concentrated in the contour convex position of the central area of the rock, as shown in Figure 15 (The red area represents the plastic zone). The total volume of the plastic zone after microwave irradiation is shown in Figure 16; the volume first increased and then decreased with the increase in roughness. The volume of the plastic zone on the flat surface was 144.83 mm³, and the plastic zone on the rough surface gradually increased by approximately 10.8%, 17.5%, 23.3%, 31.3%, 44.7%, 28.2%, and 22.9%.

The above results indicate that the change characteristics of the plastic zones of rock surfaces with different roughness values after microwave irradiation are different from their temperature characteristics and electric field characteristics. This is because the distribution of the plastic zone is not only related to the electric field, temperature, and physical and mechanical parameters; the location of the stress concentration also has a certain influence on the occurrence of the plastic zone.

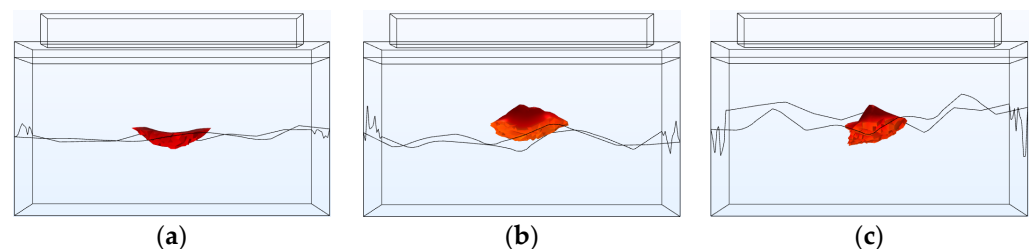


Figure 15. Cloud map of the plastic zones of the samples (Group A). (a) $R_p = 1.2$. (b) $R_p = 1.5$. (c) $R_p = 1.7$.

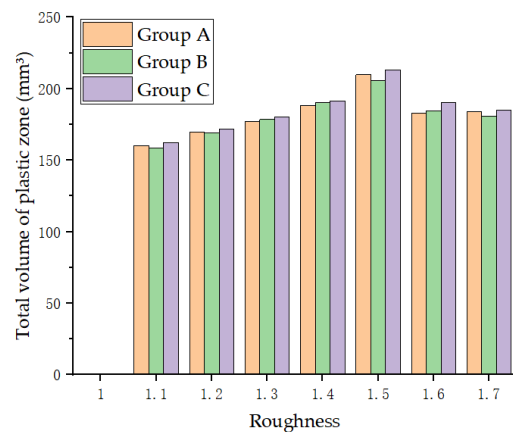


Figure 16. The total volume of the plastic zone of the samples with different roughness values after microwave irradiation.

4. Analysis and Discussion

Microwave-assisted rock breaking is the process of applying microwave irradiation to rock: The rock temperature rises to produce thermal stress, and when the stress is greater than the strength limit, the rock is damaged. This is an electromagnetic–thermal–solid multi-field coupling process. In this section, the mechanisms of the influence of rough surfaces on the effect of microwave irradiation are discussed.

When an electromagnetic wave is incident at the interface of the medium, reflection, diffraction, and refraction occur. The power flow density results indicate that the direction of the power flow density of rough surfaces changes when it reaches the surface of the sample, and the direction of the power flow density is consistent with the propagation direction of the electromagnetic wave. Thus, the incident angle of the electromagnetic wave is changed by the rough surface, and the refractive angle and the reflection angle are also altered. Table 2 presents the average results of the microwave incidence angle calculations for the whole rough surface performed in MATLAB. Calculating the reflection coefficient R through Fresnel's formula, the reflection coefficient of the flat surface was approximately 0.250, and the reflection coefficient of the specimen with a roughness of 1.5 was approximately 0.179, i.e., the electric field strength of the specimen with a flat surface and that of the sample with a roughness value of 1.5 were approximately 50% and 42.3%, respectively, indicating that the rough surface can reduce the energy loss caused by a certain electromagnetic wave reflection.

Table 2. Reflection coefficient and reflection loss for samples of each roughness value.

Roughness	Average Incident Angle (°)	Reflection Coefficient, R	Reflection Loss Rate (%)
1	0	0.250	50.0
1.1	25	0.227	47.6
1.2	34	0.209	45.7
1.3	40	0.196	44.2
1.4	44	0.187	43.2
1.5	48	0.179	42.3
1.6	51	0.175	41.8
1.7	54	0.172	41.4

When an incident wave passes through the surface of a medium, a reflected wave and a refracted wave are formed with frequencies that are the same as the incident wave; thus, reflection of the electromagnetic wave can easily cause interference between the incident wave and the reflected wave, weakening the electric field strength of the microwave. The incident wave and the reflected wave on a flat surface have the same frequency but contrasting directions and phase differences; as such, interference occurs, thereby weakening

the intensity of the incident wave. The incident wave approached the rough surface in different directions from the reflected wave, and thus, the influence of the reflected wave on the incident wave was reduced. Therefore, the loss of electric field strength was further reduced by the rough surface specimen relative to the flat surface specimen.

Solid heat transfer methods include heat conduction, convective heat transfer, and heat radiation: Convective heat transfer and heat radiation are the transfers of heat between the sample and the air, although the amount of heat transferred is small, and the influence of the two is basically negligible in microwave-irradiated rock; heat conduction is the main influencing factor. Heat flux in the x -direction of Fourier's law in heat conduction, q_x , can be calculated as follows:

$$q_x = \kappa \cdot A \cdot \frac{dT}{dx} \quad (2)$$

where κ is the thermal conductivity coefficient, $\text{W} \cdot \text{m}^{-1} \cdot \text{K}^{-1}$; A is the heat transfer area, m^2 , for temperature K ; and x is the coordinates on the thermal conduction surface, m . As shown in Figure 17, during the microwave-irradiation process, the heat conduction of the flat surface specimen was not limited to just the x and z directions, and the conduction range was hemispherical. Heat conduction at the contour convex position of the rough surface specimen was limited to the x -direction, which led to a reduction in the local heat transfer area, a decrease in the heat flux, and an observed heat accumulation effect. This caused the local temperature to be too high, and the large thermal stress destroyed the rock, thereby increasing the microwave-irradiation effect.

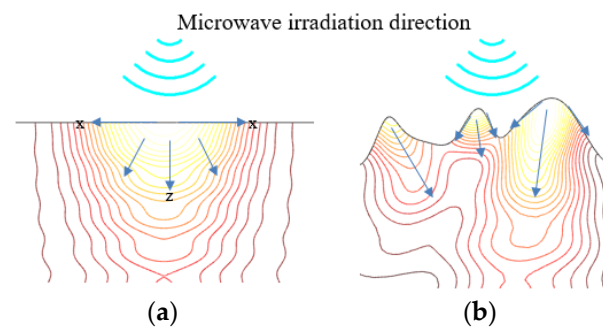


Figure 17. Heat conduction direction of different samples during microwave irradiation (Arrows are the main direction of heat transfer, and different colored lines represent different temperature gradients). (a) Flat surface. (b) Non-flat surface.

The shear stress distribution contour of the cross-section of the sample in the irradiation center area is shown in Figure 18. The maximum shear stress point of the 1.5 roughness sample appeared at the highest point of the contour convex position in the irradiation center area, whereas that of the sample with a flat surface appeared in the center of the surface: The temperature of the maximum stress point was $100\text{ }^{\circ}\text{C}$; the maximum shear stress of the flat surface sample was 22.23 MPa ; and the roughness of the 1.5 sample was 37.43 MPa . Therefore, rough surface specimen contour fluctuations are prone to stress concentrations; if the stress is large and coupled with the propagation of existing cracks, the specimen is more likely to be damaged, thereby increasing the effect of microwave irradiation rock breakage.

Analysis of the physical and numerical test results showed that the electric field strength, average temperature, and plastic zone volume of the rock surface had basically the same trend with roughness, which first increased and then decreased with the increase in roughness. A threshold between roughness values of approximately 1.4 and 1.6 was demonstrated to maximize the surface temperature, electric field strength, and plastic zone volume of the sample. Combined with the test conclusion and the influencing mechanism, there are three main reasons for the occurrence of this threshold. First, when the degree of roughness is larger, the undulating profile is larger, and the maximum difference is larger, which leads to an increase in the distance from the microwave irradiation to some positions

of the sample, and the microwave intensity decreases with the increase in irradiation distance. Therefore, when the weakening irradiation effect caused by the increase in distance increases, the influence of the rough surface on the microwave-irradiation effect is weakened. Moreover, the larger the roughness value, the larger the surface area of the sample, and thus, the area of heat conduction on the surface of the whole sample will increase, resulting in weakening of the microwave-heating effect of the entire surface. Third, with the increase in roughness, undulations of the rock surface contour will be greater, more stress concentrations are likely to occur, and the volume of the plastic zone after microwave irradiation will also be larger. However, when the roughness reaches a value of 1.5, the rock surface contour is even more undulating, and there are more convex fragments; the rock surface is thus “divided” into multiple parts by these larger contour protrusions, resulting in a reduction in the main temperature distribution area and a decrease in the plastic zone expansion area.

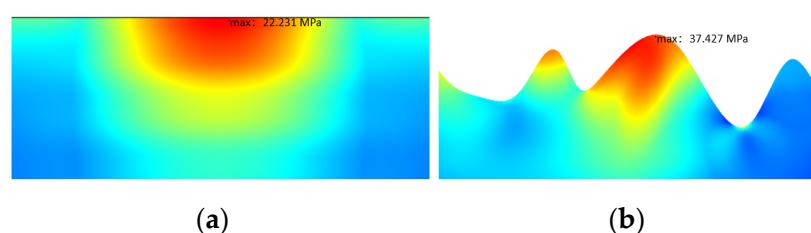


Figure 18. Shear stress distribution (The red area represents the high stress area, and the blue area represents the low stress area, maximum stress point temperature of 100 °C). (a) Flat surface. (b) Non-flat surface.

In this study, a single-mode cavity microwave oven was used to heat the rock. The microwave oven cavity was arranged with a silicon carbide plate to simulate open single-sided irradiation. However, there was still a certain discrepancy between the actual project without a cavity and completely open microwave irradiation. In order to realize the engineering applications of microwave-assisted rock breaking, an open microwave device should be used. Due to the limitations of the test equipment, the microwave-irradiation parameters selected in the test were 1 kW irradiation for 180 s, and the maximum temperature of the surface after irradiation was 229 °C. Although there were cracks on the surface of the sample after irradiation, there were no penetrating cracks or spalling, and therefore, the failure mode cannot be judged. In order to make the experimental results more instructive to actual projects, a high-power microwave device should be used.

Microwave irradiation, as an auxiliary means of mechanical rock breaking, will not directly lead to changes in mechanical parameters; however, the microwave parameters can be adjusted to achieve the best rock-breaking effect. The different roughness values studied in this experiment correspond to different tunnel faces in actual engineering, and in the case of the reasonable use of energy, different values of roughness correspond to appropriate microwave parameters required to improve the effect of microwave-assisted rock breaking.

5. Conclusions

In this study, microwave-irradiation tests were carried out on basalt samples (from Chifeng, Inner Mongolia) with surfaces of different roughness, and the influences of rough rock surfaces on the effect of microwave irradiation were explored through numerical simulation. The main conclusions are presented subsequently.

- (1) After microwave irradiation, the distribution of the high-temperature region of the flat surface sample is mainly concentrated in the central area, whereas the high-temperature area of the rough surface sample is unevenly distributed with the main high-temperature region appearing in the convex surface area. The temperature peaks

- of all rough rock surfaces were much larger than those of flat surfaces; the temperature peak increased with the increase in roughness.
- (2) When microwaves irradiate rocks, thermal stress is generated, and when the stress is greater than the strength of the rock, the rock is damaged. After microwave irradiation, no macroscopic cracks were observed on the flat surface, whereas crack propagation on the rough surface was obvious: New cracks were generated on the surface, and existing cracks continued to propagate. The P-wave velocities of the rough surface specimens were significantly reduced.
 - (3) Through numerical simulation, it was determined that the average surface electric field strength and average surface temperature of the rough surface samples were greater than those of the specimen with the flat surface. The distribution of the plastic zone is related to the distribution of the electromagnetic field and temperature; the total volume of the plastic zone increased first and then decreased with the increase in roughness.
 - (4) The comprehensive experimental and theoretical analysis shows that the influencing factors of rough rock surfaces on the effect of microwave irradiation are mainly the refraction and reflection of electromagnetic waves on the rock surface, heat conduction, and stress concentration.

Author Contributions: Conceptualization, F.C., G.L. and Z.Z.; methodology, F.C.; software, G.L. and Z.W.; formal analysis, F.C., G.L. and Z.Z.; investigation, Z.Z.; resources, Z.Z.; data curation, G.L.; writing—original draft preparation, G.L.; writing—review and editing, F.C., G.L. and Z.Z.; supervision, Z.W.; project administration, Z.Z.; funding acquisition, F.C. and Z.Z. All authors have read and agreed to the published version of the manuscript.

Funding: This research was funded by The National Natural Science Foundation of China (11872301) and The Natural Science Basic Research Program of Shaanxi Province (2020JM-453).

Institutional Review Board Statement: Not applicable.

Informed Consent Statement: Not applicable.

Data Availability Statement: The data presented in this study are available upon request from the corresponding author. The data are not publicly available due to the conduct of further research based on some of the data in this article.

Acknowledgments: The authors thank the Xi'an University of Science and Technology for their experimental and technical support.

Conflicts of Interest: The authors declare no conflict of interest.

References

1. Xu, X.H. Discussion on a New Subject of Mining Engineering-Rock Crushing Science. *Nonferrous Met* **1980**, *39*–42. Available online: https://kns.cnki.net/kcms2/article/abstract?v=ipUboLYjcOU_cYKEuLpXcboCcssuyDElFEI9Gok9zTW3sGmp1Vd2VjprVAMaB_sVBO4_mT0M-gtabtsh69rkUOTuX0ZcnXdYgKDFOMasUcQArYR_71NGdwhjiz18ya9lP-UQd5WkrY=&uniplatform=NZKPT&language=CHS (accessed on 29 November 2023).
2. Rostami, J. Performance prediction of hard rock Tunnel Boring Machines (TBMs) in difficult ground. *Tunn. Undergr. Space Technol.* **2016**, *57*, 173–182. [[CrossRef](#)]
3. Li, X.B.; Zhou, Z.L.; Wang, W.H. Development Status and Prospect of Rock Crushing Engineering. *2009–2010 Dev. Rep. Rock Mech. Rock Eng.* **2010**. Available online: https://kns.cnki.net/kcms2/article/abstract?v=ipUboLYjcOW1yGO2crL-_xalfuuCKhniTeZMI-QqDREEVhXfGX0qGTiv7ZodghYnEPoNM2x_NNp4aQBvRPqmkIqZUMKWcxVbyi3KodyVaFXoae5fAeVU5k3jGrGUW096zq6u7x8NXrInk41Qwybg==&uniplatform=NZKPT&language=CHS (accessed on 29 November 2023).
4. Lu, G.M.; Li, Y.H.; Hassani, F. Review of theoretical and experimental studies on mechanical rock fragmentation using microwave-assisted approach. *J. Geotech. Eng.* **2016**, *38*, 1497–1506.
5. Hassani, F.; Nekoovaght, P.M.; Gharib, N. The influence of microwave irradiation on rocks for microwave-assisted underground excavation. *J. Rock Mech. Geotech. Eng.* **2016**, *8*, 1–15. [[CrossRef](#)]
6. Bai, G.G.; Sun, Q.; Jia, H.L. Mechanical responses of igneous rocks to microwave irradiation: A review. *Acta Geophys.* **2022**, *70*, 1183–1192. [[CrossRef](#)]
7. Gao, M.Z.; Yang, B.G.; Xie, J. The mechanism of microwave rock breaking and its potential application to rock-breaking technology in drilling. *Petrol. Sci.* **2022**, *19*, 1110–1124. [[CrossRef](#)]

8. Kahraman, S.; Sarbangholi, F.S.; Balci, C. The effect of mineralogy on the microwave assisted cutting of igneous rocks. *Bull. Eng. Geol. Environ.* **2022**, *81*, 62–81. [[CrossRef](#)]
9. Hu, G.Z.; Zhu, J.Q.; Zhu, J. Fracturing effect and damage behaviors for microstructure in shale under microwave irradiation. *J. China Coal Sci.* **2020**, *45*, 3471–3479.
10. Liu, Z.Y.; Gan, D.Q.; Gan, Z. Experimental research on the dynamic mechanical properties and breakage behaviors of magnetite caused by microwave irradiation. *Chin. Rock Mech. Rock Eng.* **2021**, *40*, 126–136.
11. Lu, G.M.; Ding, C.; Zhou, J.J.; Liu, H.N.; Liu, C.Y. Influences of Microwave Irradiation on Rock-Breaking Efficiency of a Reduced-Scale TBM Cutter. *Appl. Sci.* **2023**, *13*, 4713. [[CrossRef](#)]
12. Chen, F.F.; Wang, C.; Zhang, Z.Q. Study of the effect of microwave irradiation path on the effectiveness of assisting rock breaking. *J. Xi'an Univ. Technol.* **2022**, *38*, 1–9. [[CrossRef](#)]
13. Li, Y.H.; Lu, G.M.; Feng, X.T.; Zhang, X.W. The influence of heating path on the effect of hard rock fragmentation using microwave assisted method. *Chin. J. Rock Mech. Eng.* **2017**, *36*, 1460–1468.
14. Lu, G.M.; Li, H.; Liu, C.; Wu, M.; Feng, A.N.; Xie, Y.Z. Influence of moisture on wave velocity and strength of rocks under microwave irradiation. *Chin. Sci. Pap.* **2019**, *14*, 1015–1021.
15. Wei, W.; Shao, Z.S.; Zhang, Y.Y. Fundamentals and applications of microwave energy in rock and concrete processing—A review. *Appl. Therm. Eng.* **2019**, *157*, 113751. [[CrossRef](#)]
16. Liu, J.; Xie, J.; Yang, B.; Li, F.; Deng, H.; Yang, Z.; Gao, M. Experimental Study on the Damage Characteristics and Acoustic Properties of Red Sandstone with Different Water Contents under Microwave Radiation. *Materials* **2023**, *16*, 979. [[CrossRef](#)]
17. Hu, G.Z.; Yang, N.; Zhu, J.; Qin, W.; Huang, J.X. Evolution characteristics of microwave irradiation on pore-permeability and surface cracks of coal with water: An experimental study. *J. China Coal Sci.* **2020**, *45*, 813–822.
18. Zhang, J.Y.; Feng, X.T.; Yang, C.X. The characteristics and mechanism of microwave-induced borehole fracturing of hard rock under true triaxial stress. *Eng. Geol.* **2022**, *306*, 106768. [[CrossRef](#)]
19. Lu, G.M.; Feng, X.T.; Li, Y.H. Influence of microwave treatment on mechanical behavior of compact-basalts under different confining pressures. *J. Rock Mech. Geotech. Eng.* **2020**, *12*, 213–222. [[CrossRef](#)]
20. Zhu, J.; Hu, G.Z.; Yang, N. Influence of microwave irradiation on the permeability of coal with different bedding dip angles. *Gas Sci. Eng.* **2022**, *103*, 104613. [[CrossRef](#)]
21. Chen, F.F.; Wu, Z.Q.; Zhang, Z.Q. Effect of Waveguide Aperture and Distance on Microwave Treatment Performance in Rock Excavation. *Sensors* **2023**, *23*, 1929. [[CrossRef](#)]
22. Khashayar, T.; Richard, C. Multiphysics study of microwave irradiation effects on rock breakage system. *Int. J. Rock Mech. Min.* **2021**, *140*, 104586.
23. Martina, P.; Jari, J.J.; Timo, S. Numerical Modelling of Microwave Heating Assisted Rock Fracture. *Rock Mech. Rock Eng.* **2022**, *55*, 481–503.
24. Ali, M.P.; Mahdi, M. Surface Roughness Assessment of Natural Rock Joints Based on an Unsupervised Pattern Recognition Technique Using 2D Profiles. *Min. Geol. Petrol. Eng. Bull.* **2023**, *38*, 185–198.
25. Ivana, D.; Petar, H.; Dražen, N. Development of a model for the estimation of shear strength of discontinuity in massive and karstified limestone. *Min Geol Petrol Eng Bull* **2021**, *36*, 43–57.
26. El-Soudani, S.M. Profilometric analysis of fractures. *Metallography* **1978**, *11*, 247–336. [[CrossRef](#)]
27. Zhao, S.X.; Xu, F.Q.; Shi, S.Z. Microwave heating of silicon carbide. *N.A. Ceram.* **1996**, *1*, 29–31.
28. Wang, Z.H.; Bai, E.L.; Liu, J.L.; Huang, H. Microwave heating efficiency and frost resistance of silicon carbide concrete. *Sci. Technol. Eng.* **2022**, *22*, 8821–8827.
29. Amin, S.; Adel, A.; Mahdi, R. Numerical and experimental analysis of fully coupled electromagnetic and thermal phenomena in microwave heating of rocks. *Miner. Eng.* **2022**, *178*, 107406.
30. Adel, A.; Amin, S.; Mahdi, R. Computational study of microwave heating for rock fragmentation; model development and validation. *Int. J. Therm. Sci.* **2022**, *181*, 107746.

Disclaimer/Publisher's Note: The statements, opinions and data contained in all publications are solely those of the individual author(s) and contributor(s) and not of MDPI and/or the editor(s). MDPI and/or the editor(s) disclaim responsibility for any injury to people or property resulting from any ideas, methods, instructions or products referred to in the content.